

# Micro-structured electrode arrays: A source of high-pressure non-thermal plasma

C. Penache<sup>\*a</sup>, C. Gessner<sup>b</sup>, A. Bräuning-Demian<sup>a,c</sup>, P. Scheffler<sup>b</sup>, L. Spielberger<sup>a,d</sup>, O. Hohn<sup>a</sup>, S. Schössler<sup>a</sup>, T. Jahnke<sup>a</sup>, K.-H. Gericke<sup>b</sup> and H. Schmidt-Böcking<sup>a</sup>

<sup>a</sup>J.W.Goethe Universität Frankfurt am Main, Germany, Technische Universität

<sup>b</sup>Braunschweig, Germany, <sup>c</sup>GSI Darmstadt, Germany, <sup>d</sup>GTZ Eschborn, Germany

## ABSTRACT

High-pressure discharges are generated using Micro-Structured Electrode (MSE) arrays with electrode distances between 50 and 250  $\mu\text{m}$ . These arrays consist either of a planar electrode system bonded to a dielectric substrate or of a matrix of holes perforated in a composite sheet made out of two metallic foils separated by an insulator. Stable discharges were produced for pressures ranging from 10 to 1000 mbar using DC and radio frequency excitation. The optical appearance is that of a homogeneous glow discharge. Spectral investigations have revealed the presence of a large number density of metastable atoms and highly energetic electrons, while the discharge has a non-thermal character. The non-equilibrium high-pressure plasma provided by the MSE arrays is suitable for surface activation, thin film deposition and reduction of pollutants.

**Keywords:** microstructures, high-pressure non-thermal plasma

## 1. INTRODUCTION

A lot of efforts were focused during the past years towards the generation of stable high-pressure discharges due to their potential industrial applications. Different approaches (corona and dielectric barrier discharges, direct current, radio frequency and microwave discharges) are known [1-4], some of them being already used on industrial scale [5, 6]. For most of the industrial applications, it is preferable to achieve stable and reliable operation of plasma sources at or only slightly below atmospheric pressure, employing moderate voltages in the range of several hundred volts. A way to generate atmospheric pressure plasma at moderate forward voltage is to scale down the electrode gap. In order to achieve breakdown at 1000 mbar in noble gases and air by applying some hundreds of volt, the distance between the electrodes needs to be in the order of 100  $\mu\text{m}$ . To this aim, Micro-Structured-Electrode (MSE) arrays have been implemented [7]. The work described below is focused on the investigation of two different types of microstructures: planar and three-dimensional MSE arrays. Electric field simulations for diverse MSE systems have shown that in the proximity of the microelectrodes the electric field is reaching values up to  $10^6$  V/cm. Such values are high enough for atmospheric pressure plasma generation but are not necessarily indicating electron field emission as discharge mechanism. Based on MSE arrays, large area DC and RF driven glow discharges can be operated at elevated pressures (10-1000 mbar) in noble gases, nitrogen and air without or with admixtures of reactive gases [8-10]. Electrical and spectral investigations performed in order to characterize the MSE sustained discharges and some of their applications will be presented.

The high-pressure plasma provided by the MSE arrays has a non-thermal character, which is very important for certain applications. These devices are suitable for gas phase plasma chemistry (reduction of pollutants) and surface processing (cleaning, activation, deposition) due to the presence of free radicals created by highly energetic electrons without heating the bulk gas. Moreover, a flexible non-planar design of the MSE allows efficient treatment of peculiar substrate shapes. High-pressure plasmas generated using structures with dimensions in the submillimetric range have been recently studied in different configurations [11-13] and their reactivity concerning gas decontamination and surface treatment was investigated. The production of excimer radiation in microdischarges operated at high pressure in rare gases and rare gas halides has been demonstrated [14, 15], making these discharges to a promising excimer source. The MSE sustained discharges are also intense sources of visible and UV radiation and they could be an alternative to conventional light sources, e.g. flat panel lamps.

\*[penache@hsb.uni-frankfurt.de](mailto:penache@hsb.uni-frankfurt.de); phone +49 69798 24294; fax +496979824212; Institut für Kernphysik, J.W.Goethe Universität Frankfurt am Main, August-Euler-Str. 6, 60486 Frankfurt am Main, Germany.

## 2. MICRO-STRUCTURED ELECTRODE (MSE) ARRAYS

Two different types of MSE have been used: planar and three-dimensional MSE. Their designs originate in microstructures currently used as position sensitive gas detectors, and known as Gas Electron Multiplier (GEM) [16] in the case of the three dimensional MSE, respectively, Micro Strip Gas Chamber for the planar MSE (MSGC) [17]. Both MSE have been optimized for high-pressure plasma generation. They consist either of a planar electrode system bonded to a dielectric substrate or of a regular matrix of holes perforated in a multilayer system (metal-insulator-metal). The distance between the electrodes needs to be around 100  $\mu\text{m}$  to allow high-pressure operation. Both the planar and three-dimensional microstructures are schematically presented in Fig. 1.

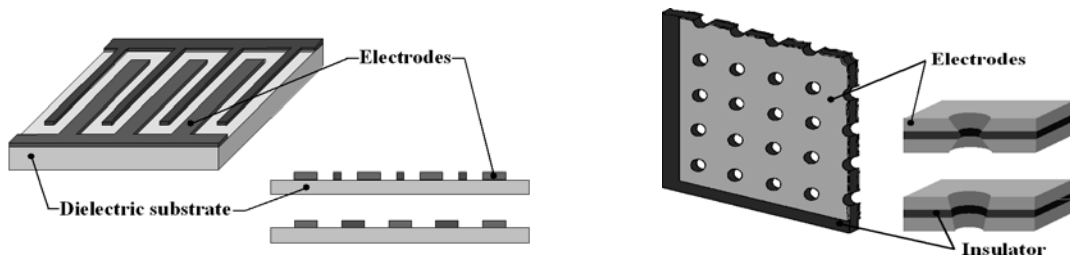


Fig. 1: Planar (left) and three-dimensional (right) Micro-Structured Electrode (MSE) arrays.

For the planar array the electrodes consist of parallel metal strips bonded to a dielectric substrate as anodes and cathodes alternately. Different metals (Cu, Au, Cr) have been used for the electrodes. Glass or ceramic have been chosen as substrates. The dimensions of the MSE array and correspondingly the discharge area were 10x10 mm<sup>2</sup>, 15x25 mm<sup>2</sup> and 50x50 mm<sup>2</sup>. The distance between the electrodes (pitch) was varied from 50 to 400  $\mu\text{m}$ , the electrode width from 20 to 400  $\mu\text{m}$  and the electrode thickness from 0.1 to 2  $\mu\text{m}$ . The following geometry was typically used in experiments: electrode gap 100  $\mu\text{m}$ , electrode width 250  $\mu\text{m}$  and metal thickness of 2  $\mu\text{m}$ . Because most of the industrial plasma applications are using nitrogen or argon as carrier gas, the MSE have been optimized for the operation in these gases where relatively high power density is required. The electrode width was increased up to 1000  $\mu\text{m}$  and the electrode gap reduced to 70  $\mu\text{m}$ . The electrode thickness was augmented to 100  $\mu\text{m}$  by copper electro-deposition. For better propagation of the electric field, the substrate between the thin electrode strips was removed by an etching process. To protect the electrodes against corrosive gases and to reduce sputtering effects the systems can be coated with a thin Al<sub>2</sub>O<sub>3</sub> film (0.5  $\mu\text{m}$ ).

The three-dimensional microstructures consist of a matrix of holes perforated in a composite sheet made out of two metallic foils separated by an insulator. Each hole can be source of a microdischarge that takes place between the two metal layers representing the electrodes. The thickness of the insulator gives the distance between the electrodes. Different materials (glass, polyimide, ceramic) with thickness ranging from 50  $\mu\text{m}$  to 250  $\mu\text{m}$  have been used for this dielectric spacer. The electrodes are made out of copper 100 to 250  $\mu\text{m}$  thick. The holes have typically diameters of 70 to 300  $\mu\text{m}$ . These perforations can have different shapes (symmetrical or not) depending on the manufacturing procedure, but no significant effect on the discharge operation was noticed as long as the hole opening is in the range mentioned above. The spacing between holes (pitch) was chosen 3 mm in order to enable the observation of individual discharges and to reduce the thermal stress on the MSE. Single-hole structures have been studied as well as arrays with up to 200 parallel-connected holes. The active surface of a plasma module with 200 holes is 50x50 mm<sup>2</sup>.

## 3. DISCHARGE OPERATION

### 3.1 Planar MSE

Using DC excitation a stable, uniform discharge covering the whole active area of the MSE array has been generated at pressures up to 80 mbar in helium and neon, respectively up to 20 mbar in argon, krypton, xenon and nitrogen. The discharge presents the electrical characteristics of a normal glow discharge. When the pressure is increased beyond the maximum values mentioned above the discharge becomes unstable. The area covered by the plasma decreases

continuously with increasing the pressure and finally the discharge contracts to a highly conductive channel. The electrodes are local strongly sputtered, leading to the destruction of the MSE array.

A stable discharge operation up to atmospheric pressure is reached when applying radio frequency (13.56 MHz) at power densities of 3-30 W/cm<sup>2</sup>. A RF power supply (ENI ACG3B) equipped with an automatic impedance matching network (ENI MW 5D) was used to provide the RF power. The experimental set-up is given in Fig. 2. The first generation MSE arrays (gap width 60-140 μm, electrode width 250 μm and electrode thickness 2 μm) are suitable to generate stable homogeneous glow discharges in helium (Fig. 3) and neon at 1000 mbar by low power densities (up to 6 W/cm<sup>2</sup>). The discharge is stable even with admixtures of reactive gases like CF<sub>4</sub> or CH<sub>4</sub> in the range of up to 10 %.

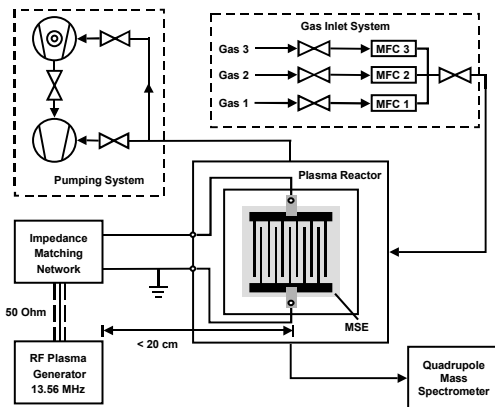


Fig. 2: Experimental set-up.

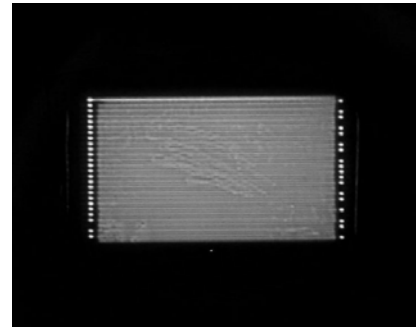


Fig. 3: RF plasma in He at 1 bar (15x25 mm<sup>2</sup>).

To operate the discharge in argon or in molecular gases like nitrogen, higher power densities of up to 30 W/cm<sup>2</sup> are necessary. Optimized MSE (electrode width 1000 μm, gap width 70 μm and electrode thickness 100 μm) allow plasma generation also in argon and nitrogen at atmospheric pressure. In nitrogen the discharge is stable and homogeneous up to a pressure of 600 mbar. Mixtures of argon and nitrogen with CF<sub>4</sub>, CHF<sub>3</sub>, and NO have been investigated as well. The optical appearance is that of a homogeneous diffuse glow discharge. The light emission is observed from a region just above the MSE with a typical thickness of 0.5 to 1.5 mm.

### 3.2 Three-dimensional MSE

Single-hole structures as well as arrays with parallel-connected holes have been mounted in a set-up similar to the one presented above. Two laterally mounted quartz windows allow the optical access to the discharge. A DC power supply TC951 was used to bias the cathode through a load resistor of 100 kΩ. Single discharges and systems of up to 200 parallel-operated discharges have been investigated as a function of the structure geometry, working gas and pressure. Stable DC glow discharges have been produced in noble gases (Ar, He, Ne), air and mixtures thereof over a wide pressure range: tens of mbar up to one atmosphere. The discharge current was varied from 0.1 to 10 mA/hole at moderate forward voltages (150-300 V). The spatial distribution of the emitted light has been recorded end-on at the cathode by a digital camera connected to an optical microscope. Simultaneously the current-voltage characteristic of the discharge was measured.

The U-I characteristic of the MSE sustained discharge (Fig. 4) is similar to the well-known characteristic of a low-pressure glow discharge and shows different modes of operation. At low current it presents a Townsend mode followed by a transition to a normal glow discharge. The Townsend regime is characterized by low charge density and electric field between the electrodes mainly axial oriented. Increasing the current, the axial electric field begins to be distorted by the space charge accumulated inside the cathode and a strong radial electric field develops. The potential distribution in the gap becomes strongly non-uniform and the cathode fall is generated. The enhanced electric field at the cathode facilitates ionization processes and correspondingly a fall in the sustaining voltage and a rise in the current is observed.

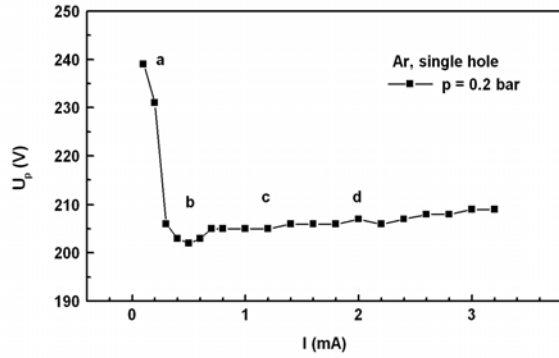


Fig. 4: Typical current-voltage characteristic of a MSE sustained DC discharge.

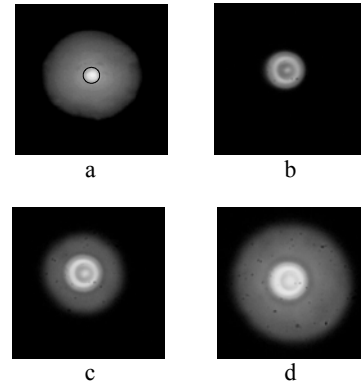


Fig. 5: Optical appearance of a microdischarge (end-on at the cathode). The black circle indicates the hole.

Accordingly, the optical appearance of the discharge changes from diffuse and relatively dark (Fig. 5a) to structured and the light emission also becomes more intensive (Fig. 5b). It suggests the presence of the luminous and dark layers known from low-pressure glow discharges. From now on the current can be increased for more than one order of magnitude at constant voltage, a typical signature for a normal glow. The discharge extends out of the hole over the cathode surface (Fig. 5c,d). Thus the active surface of the cathode is enhanced, the secondary electron emission due to ion bombardment increases and a rise in current is possible without need of higher sustaining voltage. For further rise in current an abnormal glow regime (not present in Fig. 4) has been observed. It has a resistive U-I characteristic and it is associated with the contraction of the discharge inside the hole. The operation of the discharge in the abnormal mode is usually avoided because the very high power density ( $\text{kW}/\text{cm}^2$ ) often leads to the onset of thermal instabilities and to the damage of the microstructure. The transitions between different ranges of operation as well as the reasons leading to instabilities are under investigations.

#### 4. SPECTRAL INVESTIGATIONS

The MSE sustained discharges have been investigated through optical emission spectroscopy (OES), diode laser atomic absorption spectroscopy (DLAAS) and laser induced fluorescence (LIF).

##### 4.1 Optical emission spectroscopy

OES has been performed on DC operated single-hole discharges. The chamber was coupled to a 1 m focal length scanning monochromator (Ortec model BM100) as shown in Fig. 6. A 1200G/mm grating blazed at 450 nm was used to investigate the light emission in the wavelength range 350-850 nm. An Optical Multichannel Analyzer (OMA) with 720 channels assured the detection of the spatially resolved radiation. The OMA detector consists of a photocathode, a micro channel plate system (MCP) and a diode array. The dispersion of the system was about 0.2 nm/channel.

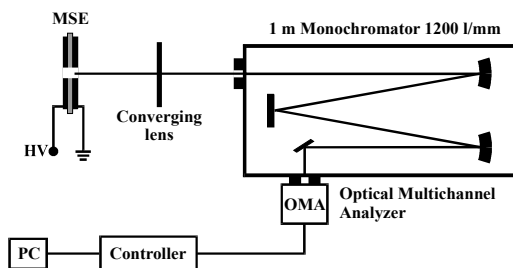


Fig. 6: Experimental arrangement used for OES.

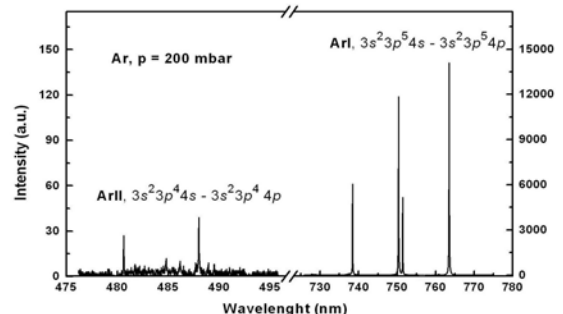


Fig. 7: Emission spectrum in Ar at 200 mbar.

The emission spectra of a microdischarge in He, Ne and Ar have been qualitatively investigated end on at the cathode respectively anode side. The light emitted from the cathode region contains the spectrum of the gas as expected for a glow discharge. Metal vapor lines of the cathode material are also present for higher discharge current (some mA). In the case of Ar, atomic transitions (ArI) between highly excited electronic states, as well as lines from single charged ions (ArII) are present as it can be seen in Fig. 7. The atomic transitions are clearly dominant. At 200 mbar the ratio ArII/ArI is about 1/1000. Increasing the gas pressure the collision frequency becomes higher and as a consequence the intensity of the ionic lines decreases. At 500 mbar the intensity of the investigated ArII lines is about 50 % from the value at 200 mbar. In the case of He and Ne only atomic lines have been observed. The lack of ionic transition can be explained by the relatively high ionization potential for He (24.59 eV) and Ne (21.56 eV) comparing to Ar (15.76 eV). Similar results have been obtained in the case of the planar MSE.

#### 4.2 Diode laser atomic absorption spectroscopy

Due to their long lifetime metastable atoms play an important role in sustaining the ionization in high-pressure non-equilibrium discharges [18], where stepwise ionization becomes important in respect to electron impact ionization. Therefore the first excited level of Ar, namely the metastable level  $1s_5$ , was investigated through DLAAS. The  $1s_5 - 2p_8$  argon transition at 801.699 nm was used. The measurements were performed on a DC operated single-hole discharge in pure Ar 200 mbar at 0.5 mA. The laser diode was centered at 801.699 nm and a wavelength range of about 40 pm was scanned with very low frequency (8 mHz) to enable the absorption profile. The wavelength calibration was given by a Fabry-Perot interferometer that has free spectral range (distance between two interference fringes) of 2 GHz. The collimated laser beam was passed through the hole, and as a consequence the integral metastable number density in the microdischarge can be evaluated. The detection of the out coming light signals (without and with plasma) was performed by a photodiode. The experimental set-up and a typical absorption signal are presented in the Fig. 8 respectively Fig. 9.

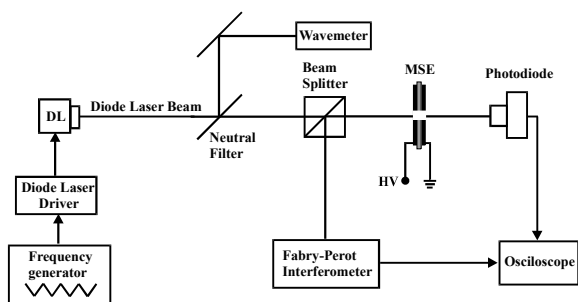


Fig. 8: Experimental set-up for DLAAS performed on a single microdischarge.

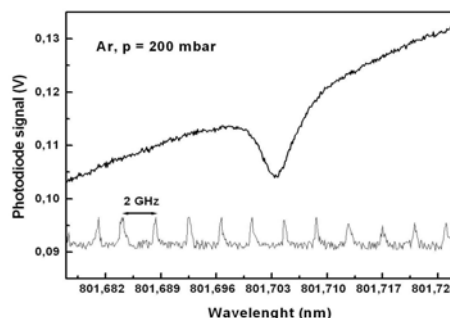


Fig. 9: Absorption signal at 801.699 nm in Ar, 200 mbar and interference fringes.

From these measurements the population of the Ar  $1s_5$  metastable level was estimated at  $5 \times 10^{12} - 10^{13} \text{ cm}^{-3}$ . Due to the high number density of metastable atoms produced in the microdischarge, the DLAAS technique can be successfully used to investigate the MSE plasma, in spite of the very short absorption length. Plasma parameters like gas temperature and electron number density can be evaluated from the analysis of the absorption profiles, taking into account the significant broadening mechanisms. Estimation of the above mentioned plasma parameters from the detailed study of different metastable and resonant levels, is envisaged.

#### 4.3 Laser induced fluorescence

Species in the electronic ground state under equilibrium conditions can be characterized by state selective excitation to an excited electronic state and observation of the total fluorescence light. State selective excitation can be achieved by using laser radiation. LIF investigations have been performed on DC operated planar MSE at relatively low pressure in a He/500 ppm NO mixture to determine the gas temperature. The experimental set-up (Fig. 10) was outlined for the detection of the  $A^2\Sigma^+ \rightarrow X^2\Pi_{1/2}$  transition of NO.

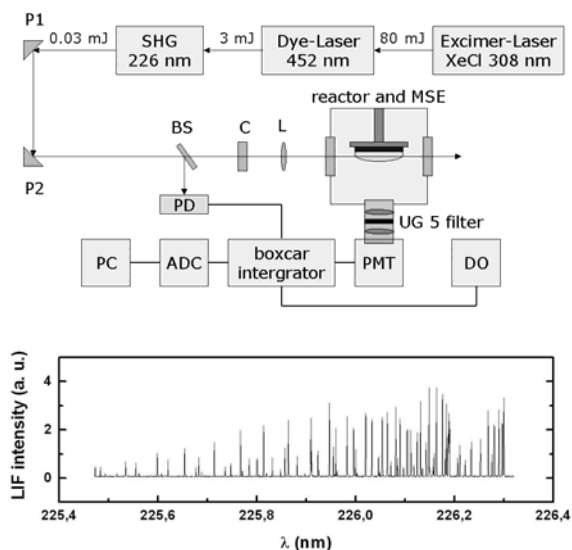


Fig. 10: Experimental set-up for LIF investigations and a measured fluorescence spectrum.

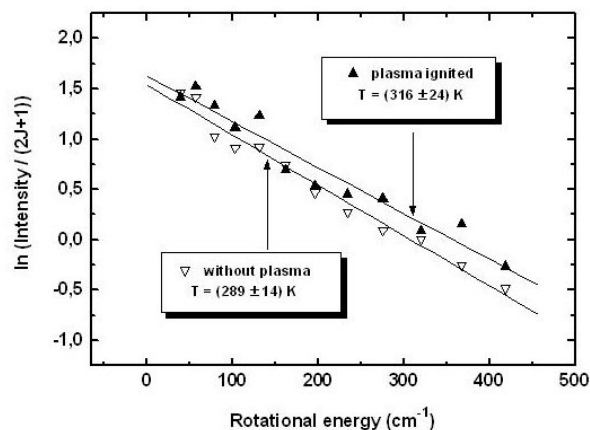


Fig. 11: Boltzmann diagram for the  $R_1$  branch of the (0, 0) band of the  $A^2\Sigma^+ \rightarrow X^2\Pi_{1/2}$  electronic transition of NO.

Tunable laser light probed the discharge volume a few mm above the MSE surface. The laser excitation wavelength was scanned from 225.5 nm to 226.4 nm. The UV laser radiation is obtained by second harmonic generation of the radiation emitted by a tunable pulsed dye laser operated at Coumarin 47 and pumped by a XeCl excimer laser. The laser beam is expanded using a combination of cylindrical and converging lenses to form a laser sheet. The emitted fluorescence light was detected at  $90^\circ$  by a photomultiplier. The out coming signal was monitored by means of a digital oscilloscope and was submitted to a gated integrator and boxcar averager which was triggered by a photo diode. Finally the signal was transferred to a personal computer with an A/D-converter. A LIF spectrum of the  $A^2\Sigma^+ \rightarrow X^2\Pi_{1/2}$  transition of NO is presented in Fig. 10. All observed lines can be assigned to the rotational transitions belonging to the  $R_1$ ,  $R_{21}$  and  $Q_1$  branches of the (0, 0) band of the  $A^2\Sigma^+ \rightarrow X^2\Pi_{1/2}$  electronic transition. The rotational lines of the  $R_1$  branch are well resolved and therefore are used to determine the gas temperature  $T$  according to  $I \sim S_{J,J''} \cdot (2J''+1) \cdot \exp(-E_{rot}/kT)$ , where  $I$  is the intensity of lines belonging to the  $R_1$  branch and  $E_{rot}$  the rotational energy of the lower  $J''$  state. Under Local Thermodynamic Equilibrium (LTE) conditions a semi-logarithmic plot of the intensity of different rotational lines versus the rotational energy is a straight line with the slope yielding  $1/T_{rot}$ . The temperature obtained without plasma  $T = 289 \pm 14$  K corresponds to room temperature. When the discharge is ignited the temperature  $T = 316 \pm 24$  K is only slightly higher (Fig. 11). In order to prove the values resulted from the Boltzmann diagram, the experimentally measured spectrum was compared with calculated spectra for different temperatures and the best fit was obtained for  $T = 300$  K.

## 5. APPLICATIONS

The high-pressure MSE sustained discharges discussed in previous sections have characteristics that recommend them for non-thermal plasma processing, e.g. surface treatment and plasma chemistry. In special configurations they can provide well-directed remote plasma.

### 5.1 Thin carbon film deposition

By using planar MSE with radio frequency excitation, thin carbon films have been deposited using mixtures of 5 % methane ( $\text{CH}_4$ ) and 2 % acetylene ( $\text{C}_2\text{H}_2$ ) in helium at a pressure of 10 to 100 mbar [19]. The substrate was placed parallel with the MSE at a distance of 9 mm. A pulsed bias voltage of 550 Vpp at 9.5 kHz was applied to the substrates. The deposition time was varied between 10 and 30 minutes by a RF power of 30-40  $\text{W}/\text{cm}^2$ . Carbon films with a thickness of 5 to 10  $\mu\text{m}$  and a hardness of about 9000 MPa have been deposited on various substrates (silicon, glass, aluminium, copper). By optimizing deposition parameters like gas mixture/flow, time and distance the quality of the film can be further increased.

## 5.2 Waste gas treatment

Experiments have been performed to demonstrate the decomposition of exhaust gases at pressures up to one atmosphere. To study the reactivity of the MSE plasma regarding decomposition of exhaust from diesel engines and waste gas from the semiconductor industry the following systems are under investigation: mixtures of NO in helium [20], argon and nitrogen, respectively mixtures of CF<sub>4</sub> and CHF<sub>3</sub> in helium and nitrogen.

In the case of radio frequency operated MSE in a He/CF<sub>4</sub> mixture at 250 mbar for RF power of 42 W/cm<sup>2</sup>, CF<sub>4</sub> can be decomposed up to 20 % leading to the formation of HF, CO<sub>2</sub>, COF<sub>2</sub>, COF<sup>+</sup> and CN<sup>+</sup>.

For He/500 ppm NO mixtures decomposition rates of up to 65 % are obtained at RF power density of 5 W/cm<sup>2</sup> and gas flow of 290 sccm. The concentrations of some molecules of interest (N<sub>2</sub>, O<sub>2</sub>, NO and NO<sub>2</sub>) are monitored by a quadrupole mass spectrometer (Fig. 2). A mass spectrum, measured in the Multiple Ion Detection mode (MID) is presented in Fig. 12. As long as the discharge operates there is a removal of NO and NO<sub>2</sub>. Simultaneously the concentration of molecular and atomic oxygen and of atomic and molecular nitrogen increases showing that the main products are N<sub>2</sub> and O<sub>2</sub>. The formation of higher nitrogen oxides (NO<sub>3</sub>, N<sub>2</sub>O<sub>3</sub>, N<sub>2</sub>O<sub>5</sub>) was not detected. When the plasma is turned off the decomposition process stops and the NO concentration rises up to its initial level. By increasing the RF power density from 3 to 5 W/cm<sup>2</sup>, the removal efficiency increases as it can be seen in Fig. 13. In Ar/NO mixtures the decomposition rate is about 30% at a gas flow of 250 sccm, being smaller than in He/NO mixtures. Furthermore, in these mixtures using a very low gas flow (5-10 sccm) an enhancement in the NO concentration was noticed. The removal efficiency depends also on the retention time of the pollutant in the active volume, thus by increasing the gas flow up to 1000 sccm the NO<sub>x</sub> decomposition efficiency decreases.

In the case of the three-dimensional MSE, DC operated at atmospheric pressure, the removal efficiency of NO in helium plasma with 500 ppm NO admixture is about 30% at a power consumption of 0.4 W/microdischarge and is proportional to the discharge power. The removal efficiency can be increased by increasing the power density in the active volume or by switching on more microstructures successively.

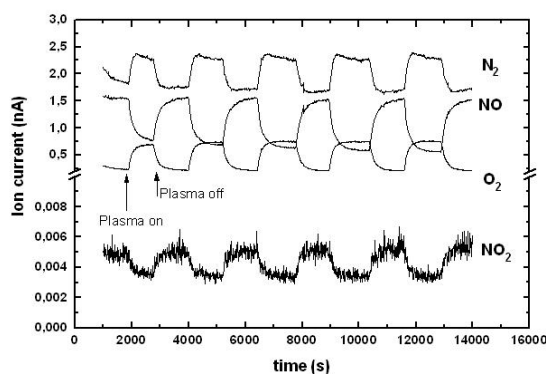


Fig. 12: NO decomposition in a planar MSE discharge at 1 bar in He/NO 500 ppm mixture.

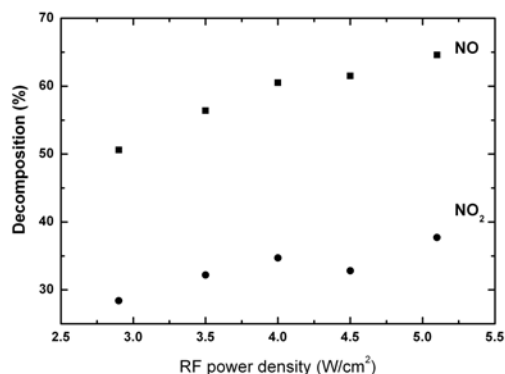


Fig. 13: Dependency of the NO<sub>x</sub> removal efficiency on the discharge power density.

## 5.3 Plasma chemistry

Different plasma enhanced syntheses can be carried out in proving that the MSE sustained discharges are suitable as a catalyst for chemical processes. CH<sub>4</sub> and C<sub>2</sub>H<sub>2</sub> have been decomposed to form higher hydrocarbons (C<sub>2</sub>H<sub>3</sub>, C<sub>2</sub>H<sub>5</sub>, C<sub>3</sub>H<sub>3</sub>, C<sub>3</sub>H<sub>7</sub>) with decomposition ratios of up to 60 %, using mixtures of 5 % CH<sub>4</sub> and 2 % C<sub>2</sub>H<sub>2</sub> in He as process gases. NO, to quote another example, may be produced in MSE discharges generated in air. The generation of small, well-defined quantities of NO is very important for medical studies. The discharge is electrically steerable and thus, the product concentration is adjustable, depending on the power applied to the microstructure. Furthermore, because of their dimensions, the MSE arrays are ideally applicable as catalyst in micro-reactors.

## 5.4 Supersonic plasma jet

Apart from the quasi-static operation described above, the three-dimensional MSE can be operated with massive gas flow, as a plasma jet. Pure gases or gas mixtures flow through a single hole from a high-pressure side ( $p_{\text{high}} = 500$  mbar up to several bar) to a low-pressure side ( $p_{\text{low}} < 10^{-2}$  mbar). In this operation mode the discharge can be ignited in the hole and different active species produced in the discharge can be extracted (remote plasma) and used for different applications, e.g. surface activation. The pressure difference between the two volumes separated by the MSE will influence the retention time of the gas in the active discharge volume and therefore the characteristics of the extracted particles. For special pressure ratios ( $p_{\text{high}} / p_{\text{low}}$ ) a supersonic jet is produced and the gas is cooled by adiabatic expansion into vacuum. The directional beam is well localized and transversal temperature in the range of mK can be reached. The special discharge geometry (hole diameter 50 to 300  $\mu\text{m}$ ) and operation parameters combined with the adiabatic expansion result in a versatile source for excited/metastable atoms, ions, etc. The main advantage is that the entire gas is flowing through the active volume. By varying the pressure ratio and the gas flow the source can be optimized for different applications. A diaphragm (skimmer) can be used to reduce the pressure behind the first stage and form a fine beam with a typical diameter of less than 1 mm. Typical operation pressures for this configuration are  $10^{-3}$  mbar in the first stage and  $10^{-6}$  mbar behind the skimmer. The experimental set-up is depicted in Fig. 14. This set-up is very suitable as ion source for singly charged ions [21]. The main part of the source, represented by the MSE and a special housing is very compact and is driven by a moderate voltage (less than 1000 V). For two different working gases the total extracted ion current as a function of the discharge current is presented in Fig. 15. The extracted species can be analyzed using deflection methods and position sensitive detectors.

Furthermore, a similar set-up can be employed as a part of a spin-polarized  $\text{He}^*$  target for atomic physics experiments. The MSE plasma is used as source of metastable ( $^3\text{S}_1$ ) He. The target is not yet completely characterized, but due to cooling with liquid  $\text{N}_2$  and by taking advantage of supersonic expansion, a high quality  $\text{He}^*$  beam [22] can be produced. The yield of  $^3\text{S}_1$ -He is expected to be comparable with that of existing  $\text{He}^*$  sources.

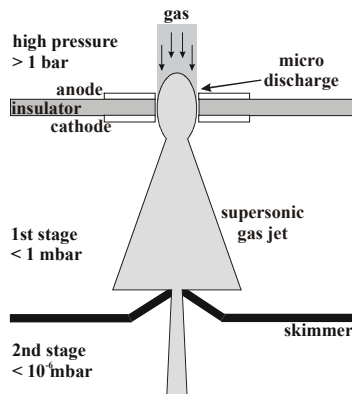


Fig. 14: The experimental set-up used for the generation of a DC plasma jet.

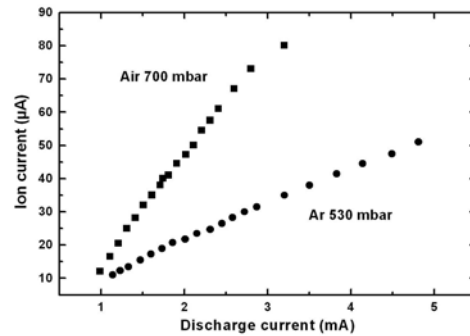


Fig. 15: The total ion current extracted from the MSE sustained plasma.

## 6. CONCLUSIONS

The MSE sustained discharges are combining the advantage of high pressure with the non-thermal character. The optical appearance shows a stable, homogeneous glow discharge for pressures ranging from 10 to 1000 mbar using DC and radio frequency excitation. Spectral investigations have revealed the presence of a large number density of metastable atoms and highly energetic electrons. DC parallel operation of up to 200 microdischarges without individual ballast was proven in rare gases for pressures up to 300 mbar. Systems of resistively decoupled microdischarges were successfully operated at atmospheric pressure. Current densities from 0,5 to 100  $\text{A}/\text{cm}^2$  respectively power densities of about 0,1 to 25  $\text{kW}/\text{cm}^2$  have been reached. Stable, non-filamentary RF discharges up to  $50 \times 50 \text{ mm}^2$  have been produced at atmospheric pressure using planar MSE. The power density can vary between 3 and 40  $\text{W}/\text{cm}^2$  depending on the working gas and the active area of the microstructure.



Surface treatment on industrial scale requires large area uniform discharges. When planar MSE are chosen this is realized by parallel arrangements of microstructures, building a plasma module. In the case of three-dimensional MSE, large area is achieved by running a large number of microdischarges in parallel with or without resistive decoupling. Homogenous plasma can be obtained by increasing the holes density to about 500 holes/cm<sup>2</sup>. Another approach is to use the MSE discharge as “plasma cathode” for a high-pressure glow discharge created between the microstructure and an additional electrode [23]. If the substrate to be treated is metallic can play itself the role of the additional electrode. For special applications, when local and directed surface activation is desired a single-hole discharge can be operated under static conditions or as a plasma jet. The MSE plasma source is an ideal device for surface treatment, because it can be individually adapted even to curved or less accessible surfaces, if the electrode system is bonded to a flexible substrate [24]. Concerning waste gas purification and plasma chemistry, it was demonstrated that both planar and three-dimensional MSE arrays could be implemented as a versatile gas filter at atmospheric pressure.

## ACKNOWLEDGMENTS

The authors like to thank Dr. K. Frank and Dr. U. Ernst (University of Erlangen, Germany), Dr. K. Niemax and Dr. J. Franzke, (ISAS Dortmund, Germany) for fruitful discussions and providing equipment for the OES and DLAAS investigations. Special thanks are addressed to Dr. M. Miclea, (ISAS Dortmund, Germany) for support in performing the DLAAS measurements. This work was supported by: Bundesministerium für Bildung und Forschung (BMBF), Verein Deutsche Ingenieure (VDI), Deutsche Bundesstiftung Umwelt and Land Hessen. Cooperation partners: Hamon Rothemühle Cottrell GmbH, Robert Bosch GmbH, Roentdek GmbH.

## REFERENCES

1. S. Okazaki, M. Kogoma, M. Uehara, Y. Kimura, *J. Phys. D: Appl. Phys.* **26**, pp. 889-892, 1993.
2. E. E. Kunhard, K. H Becker, US Pat. No.5,872,426 (1999).
3. J. Reece Roth, US Pat. No.5,938,854 (1999).
4. M. Mildner, D. Korzec, J. Engemann, *Surface and Coatings Technol.* **112**,pp. 366-372, 1999.
5. Yu. P. Raizer, *Gas discharge physics*, Springer, Berlin, 1997.
6. J. Reece Roth, *Industrial plasma engineering: Applications to nonthermal plasma processing*, Institute of Physics, 2001.
7. M. Roth, T. Haas, M. Lock, K.-H. Gericke, A. Bräuning-Demian, L. Spielberger, H. Schmidt-Böcking, *Proc. of 1<sup>st</sup> Int. Conf. on Microreaction Technology*, Springer, Berlin, pp. 62-69, 1998.
8. C. Penache, A. Bräuning-Demian, L. Spielberger, and H. Schmidt-Böcking, *Proc. of Hakone VII*, Greifswald, pp. 501-505, 2000.
9. A. Bräuning-Demian, L. Spielberger, C. Penache, H. Schmidt-Böcking, *Proc. of the XIII Int. Conf. on Gas Discharges and their Applications*, Glasgow, pp.426-429, 2000.
10. C. Geßner, P. Scheffler, K.-H. Gericke, *Proc. of the XIII Int. Conf. on Gas Discharges and their Applications*, Glasgow, pp. 548-551, 2000.
11. J. W. Frame, J. G. Eden, *Electr. Lett.* **34** (15), pp. 1529-, 1998.
12. W. Shi, R. H. Stark, K. H. Schoenbach, *IEEE Trans. Plasma Sci.* **27**, pp. 16-17, 1999.
13. L. D. Biborosch, O. Bilwatsch, S. Ish-Shalom, E. Dewald, U. Ernst, K. Frank, *Appl. Phys. Lett.* **75** (25), pp. 3926-3928, 1999.
14. A. El-Habachi, K. H. Schoenbach, *Appl. Phys. Lett.* **72** (1), pp.22-24, 1998.
15. A. El-Habachi, W. Shi, M. Moselhy, R. H. Stark, K. H. Schoenbach, *J. Appl. Phys.* **88** (6), pp. 3220-3224, 2000.
16. F. Sauli, *Nucl. Instr. Meth. A* **386**, pp. 531-534, 1996.
17. A. Oed, *Nucl. Instr. Meth. A* **236**, pp. 263-266, 1988.
18. F. Massines, A. Rabehi, P. Decomps, R. B. Gadri, P. Segur, C. Mayoux, *J. Appl. Phys.* **83**, pp.2950-2957, 1998.
19. C. Geßner, P. Scheffler, K. H. Gericke, *Proc. of the 25<sup>th</sup> Int. Conf. on Phenomena in Ionized Gases (ICPIG)*, Nagoya, **4**, pp.151-152, 2001.
20. P. Scheffler, C. Geßner, K.-H. Gericke, *Proc. of Hakone VII*, Greifswald, pp. 407-411, 2000.
21. S. Schössler, T. Janke, O. Hohn, C. Penache, A. Bräuning-Demian, H. Schmidt-Böcking, to be published.
22. J. Kawanaka, M. Hagiuda, K. Shimuzu, F. Shimuzu, H. Takuma, *Appl. Phys. B* **56**, pp. 21-24, 1993.
23. R. H. Schoenbach, R. H. Stark, *Appl. Phys. Lett.* **74**, pp. 3770-3772, 1999.
24. J. Wallace, *Laser Focus World*, pp. 32-38, 2000.